Electronic Structure and Properties of FeO_n and FeO_n^- Clusters

Gennady L. Gutsev,* S. N. Khanna, B. K. Rao, and P. Jena

Physics Department, Virginia Commonwealth University, Richmond, Virginia 23284-2000

Received: March 15, 1999; In Final Form: May 19, 1999

The electronic and geometrical structures of the ground and some excited states of the FeO_n and FeO_n^- clusters ($n = 1-4$) have been calculated using the density-functional theory with generalized gradient approximation for the exchange-correlation potential. It is found that the multiplicity of the ground states decreases with increasing n, and the ground states of FeO^- and FeO_2^- are quartets whereas those of FeO_3^- and FeO_4^- are doublets. All of these anions possess isomers with different spatial or spin symmetries that are close in energy to their ground states. For example, FeO_4^- has at least five stationary states that are stable against electron detachment and fragmentation. Our calculated adiabatic electron affinities (A_{ad}) of FeO, FeO_2, and FeO_3 are within 0.2 eV of the experiment. FeO_4 was found to be a particularly interesting cluster. Although its neutral precursor possesses a closed electronic shell structure, it has an A_{ad} of 3.8 eV, which is higher than the electronic affinity of halogen atoms. The experimental estimate of 3.3 eV for the A_{ad} of FeO_4 is shown to originate from the detachment of an electron from one of the higher-energy isomers of the FeO_4^- cluster. The energetically preferred dissociation channels of FeO_2, FeO_3, FeO_4, FeO_3^-, and FeO_4^- correspond to abstraction of an O_2 dimer but not to an Fe−O bond rupture. FeO_3^- and FeO_4^- are found to be thermodynamically more stable than their neutral closed-shell parents, and FeO_3^- is the most stable of all the clusters studied. The existence of several low-lying states with different multiplicities in FeO_n and FeO_n^- indicates that their magnetic properties may strongly depend on temperature.

Introduction

The observation of high-temperature suprerconductivity in rare earth copper oxides, giant magnetoresistance in complex manganese oxides[1,2] and the recent discovery of resonant quantum tunneling[3] in $Mn_{12}O_{12}$ has revived an interest in 3d metal oxides. The bulk transition metal oxides are characterized by different metal−oxygen bonding, which depends on the metal to oxygen content. Depending on this content, transitions from metallic to insulating and from paramagnetic to ferromagnetic behavior are observed.

While bulk oxides exist for certain metal to oxygen ratios, this ratio can be varied over a wider range in clusters. This has generated considerable interest in studies of small transition metal oxygen clusters and their ions. Among these, studies of iron oxide clusters are particularly important not only because the interaction of iron with oxygen is of great interest in understanding corrosion but also because iron oxide plays a central role in the transport of oxygen in biological systems. Recently, Wang and his group[4] have obtained the photoelectron spectra of a number of transition metal anions including iron oxide anions FeO_n^- ($n = 1-4$)[5,6] using lasers with 3.49 and 4.66 eV photon energies. Prior to their measurements, only FeO^- was studied[7,8] by laser photodetachment spectroscopy with 2.52 eV photons. Although features of these spectra have been discussed[9] on the basis of qualitative considerations of oxidation tendencies and a simple electrostatic model, no accurate quantum-mechanical computational studies have been reported on the structure of oxide anions FeO_n^-. Theoretically, the geometry and vibrational frequency of the ground state of FeO^- have been studied with the use of nonempirical pseudopotentials.[10] The vertical detachment energy of an electron from FeO_4^- has been calculated[11] by the discrete-variational X_α method assuming a tetrahedral geometry taken from solid salts containing iron tetraoxide units which are considered to be $[FeO_4]^{2-}$ dianions.[12] The latter dianion has also been studied by the scattered-wave X_α method[13] and local-density approximation of the density-functional theory (LDA-DFT).[14,15]

The neutral iron oxides have received much more attention, especially iron monoxide, whose properties have been the subject of numerous experimental[16−22] and theoretical investigations.[10,23−27] For iron dioxide, infrared spectra were recorded by several groups[28−31] and the infrared spectra of FeO_3 and FeO_4 have been measured by Andrews et al.[32] Theoretical calculations on FeO_n for $n > 1$ are scarce: some configurations of FeO_2 and FeO_3 were optimized using the generalized-gradient approximation for the exchange-correlation potential within the DFT theory.[33] Calculations on the ground states of FeO_2, FeO_3, and FeO_4 and their isomers were performed at different levels (less accurate for FeO_3 and FeO_4) to help in the assignment of experimental infrared spectra.[32] While the ground-state symmetry of FeO_3 has been found to be the same ($^1A_1'$, D_{3h}) in both studies,[31,33] different spatial symmetries have been obtained for FeO_2: $^3B_1$ in ref 32 but $^3B_2$ in ref 33 with rather different bond angles.

In view of the scarcity of experimental data on the structure of gas-phase iron oxides and its anions, it is useful to have an insight into the nature of their geometric, electronic, thermodynamic, and magnetic properties obtained in a consistent manner within the same reliable calculational approach. The aim of this work is to perform a detailed study for iron oxides: FeO_n and FeO_n^- ($n \leq 4$) within the DFT formalism using the exchange-correlation functional given by a combination of the Becke's exchange[34] and Perdew−Wangs' correlation[35] gradient-corrected functionals. This approach has proven to be successful

10.1021/jp9909006 CCC: $18.00
Published on Web 07/02/1999

in explaining optically induced magnetism in cobalt iron cyanide[36] and electron affinities of MnO_n, $n \leq 4$, within 0.2 eV.[37]

In this paper, we have calculated the preferred spin multiplicities and ground-state geometries of both neutral and negatively charged iron oxides having made an extensive search among different geometrical configurations and spin multiplicities. Such a search also provides the structure of isomers within the same spin multiplicity. In addition, we have computed the adiabatic electron affinities for the neutral species and compare them to experimental data. Finally, we estimate the thermodynamic stability of both FeO_n and FeO_n^- series of clusters.

Computational Details

The calculations are performed using the molecular orbital theory where a linear combination of atomic orbitals centered at various atomic sites constitutes the cluster wave function. For the atomic orbitals we have used the standard 6-311+G* basis (Fe [10s7p4d1f]; O [5s4p1d]). The many-electron potential is constructed by using the density-functional theory with the generalized gradient approximation for the exchange-correlation functional. We have used Becke's exchange[34] and Perdew−Wangs' correlation[35] functionals, referred as to BPW91 below, in the Gaussian94 software.[38] One of the difficulties associated with transition metal elements is their open d shell structure. The d electrons are quasi-localized and a cluster containing transition metal atoms has many spin-multiplet structures within a narrow energy range. Thus obtaining the spin multiplicity of the ground state is a nontrivial problem.

Originally, Kohn and Sham[39] have formulated the DF theory for the ground states. It has been proven later[40,41] that the DF theory can be extended also for the lowest energy states in each particular symmetry (spatial and spin) channel. We have performed extensive optimizations beginning with different atomic configurations for each spin multiplicity for both FeO_n and FeO_n^- series. In each case, the geometry optimization was carried out by examining the gradient forces at each atomic site and moving the atoms along the path of steepest descent until the forces vanish. We feel confident that we are able to arrive at the ground-state configurations.

Since the spin multiplicity of a cluster and the distribution of the electron spin densities among various atomic sites play an important role in the ground state of a cluster, we briefly review the difficulties associated with density-functional and Hartree−Fock based theories in accounting for magnetic moments. In conventional density-functional theory, neither the orbital angular momentum $\hat{L}$ nor spin angular momentum $\hat{S}$ operators are defined. The relationship between the spin multiplicity $M = 2S + 1$, and the number of electrons in the spin-up (n_α) and spin-down (n_β) is given by

$$2S = \int [\rho^\alpha(\mathbf{r}) - \rho^\beta(\mathbf{r})]\, d\mathbf{r} = n_\alpha - n_\beta \qquad (1)$$

where ρ^α and ρ^β are the electronic densities for electrons with α (up) and β (down) spins. The total density $\rho(\mathbf{r}) = \rho^\alpha(\mathbf{r}) + \rho^\beta(\mathbf{r})$ corresponds to a pure wave function satisfying the condition $\hat{S}^2\Psi = S(S+1)\Psi$.

Within the unrestricted Hartree−Fock (UHF) formalism, which corresponds to a spin-polarized density-functional variant, the resulting approximate wave function is generally not an eigenfunction of $\hat{S}^2$ or $\hat{S}_z$ and contains some so-called spin contamination. It was shown[42] that for the N-electron system ($N = n_\alpha + n_\beta$) the following equation holds

$$\langle S^2 \rangle = -\frac{N(N-4)}{4} + \int \Gamma(\mathbf{r}_1 s_1, \mathbf{r}_2 s_2 | \mathbf{r}_1 s_2 \mathbf{r}_2 s_1)\, d\mathbf{x}_1\, d\mathbf{x}_2 \qquad (2)$$

where $\mathbf{x}_i = (\mathbf{r}_i \sigma_i)$ is the space-spin coordinate of the i the electron and Γ is the two-particle density normalized to $N(N-1)/2$. Evaluation of $\hat{S}^2$ within post-HF computational methods is relatively straightforward,[43,44] but it is complicated in DFT methods since the two-particle density is not defined. Several schemes for approximate estimations of $\langle \hat{S}^2 \rangle$ have been suggested[45] on the basis of use of one-particle densities combined with correlation hole functions. The simplest way of evaluating $\langle \hat{S}^2 \rangle$ is to construct an approximate wave function using one-electron orbitals obtained from a self-consistent solution to the Kohn−Sham equations[39] (see, e.g., refs. 46 and 47) and then using standard schemes for evaluating the spin contamination for a UHF function. This is implemented in the Gaussian94 package and others. Generally, Kohn−Sham orbitals provide wave functions with a much smaller spin contamination than the UHF ones do.[48]

The total magnetic moment in the Russell−Saunders scheme is defined as $\boldsymbol{\mu} = -\mu_B(\hat{L} + 2\hat{S})$,[49] where μ_B is the Bohr magneton. Within the Heisenberg model, one neglects $\hat{L}$ contributions and defines $\boldsymbol{\mu} = g\mu_B\hat{S}$, where g is close to the "spin-only" value of 2. To evaluate local magnetic moments at atom cites, one can use the Mulliken scheme for partitioning the electron density between atoms[50] or a natural bond analysis (NBO), which is based on the use of localized orbitals constructed from the occupancy-weighted symmetric orthogonalized natural atomic orbitals.[51] The NBO analysis provides effective atomic configurations for each atom in the cluster, and one can evaluate the local magnetic moment of a particular atom by subtracting α and β natural populations.

In the case of iron oxides, both Mulliken and NBO schemes provide nearly the same charges and local magnetic moments. As a typical example, let us consider the results for the ground state of FeO. The magnetic moments calculated using the Mulliken population analysis are 3.5 and 0.5 μ_B at the Fe and O sites, respectively, and the NBO analysis provides 3.4 and 0.6 μ_B, correspondingly. Experimental magnetic moments at atomic sites are available generally for solids. Zheng[52] has computed local magnetic moments at Ni in NiO using an embedding cluster technique. His calculated value of 1.91 μ_B agrees well with experimental values that range from 1.64 to 1.90 μ_B. This agreement as well as the closeness of magnetic moments obtained from the Mulliken and NBO analyses lends credibility to the use of Mulliken analysis for calculating local magnetic moments.

We should also mention that recently a hybrid Hartree−Fock density-functional-theory (HFDFT)[53−56] method where the exchange-correlation functional[57,58] is given by

$$V_{xc} = (1-A)E_x^{Slater} + AE_x^{HF} + BE_x^{Becke} + CE_c^{LYP} + (1-C)E_c^{VWN} \qquad (3)$$

has been used as an alternative approach to the BPW91 method described earlier. This hybrid method commonly referred to as B3LYP. In eq 3, E_x^{Slater} is the classical Slater exchange,[59] E_x^{HF} is the HF exchange, E_x^{Becke} is a gradient correction to the exchange introduced by Becke,[34] E_c^{LYP} is the Lee−Yang−Parr correlation potential,[60] and E_c^{VWN} is the Vosko−Wilk−Nusair correlation potential.[61] A, B, and C are the constants obtained by Becke[57] when fitting the theoretical results to the experimental heats of formations. This method allows a rather good description of compounds containing main-group elements,[62,63]

but it provides poor estimates for the A_{ad} of such "test" molecules as CN[63] or SF_6.[64] For example, the A_{ad} of CN computed using the BLYP method is 4.56 eV[54] while the experimental value is 3.82 eV.[65] In contrast, using the BPW91 approach, we calculate the A_{ad} of CN to be 3.77 eV in excellent agreement with experiment.

We should point out that we have performed calculations for FeO and FeO^- using the B3LYP procedure and 6-311+G* basis set. The results are disappointing: FeO states with multiplicities 5 and 7 are nearly degenerate in energy. Moreover, the latter is lower by 0.01 eV and should be assigned as the ground state in contradiction with experiment. The spectroscopic constants of FeO ($2S + 1 = 5$) computed with this approach ($R_e = 1.668$ Å and $\omega_e = 808$ cm^{-1}) are in rather poor agreement with experiment[66] (1.616 Å and 881 cm^{-1}, respectively). The A_{ad} of FeO is 2.23 eV, which again is well above the experimental value[7] of 1.49 eV. A similar trend for B3LYP to favor high-multiplicity states was observed for FeO_2 as well.[31] It is for this reason, all our following calculations are done at the BPW91 level of theory. Currently, there are no experimental techniques that can measure the magnetic moments at a given atomic cite in a gas-phase cluster. However, the total energies of the neutral and charged clusters corresponding to the ground-state multiplicities can be used to study the electron affinities, ionization potentials, and fragmentation energies for which experimental data are available. A good agreement between theory and experiment then validates the accuracy of the calculations and interpretation of the cluster's atomic and electronic structure. We have calculated the electronic affinities, vibrational frequencies and fragmentation energies of FeO_n and FeO_n^- clusters. In the following, we present these results.

Results and Discussion

This section is divided into several parts where we discuss (a) the equilibrium geometries, (b) charges on atoms and spin distributions, (c) vibrational frequencies, (d) electron affinities, and (e) thermodynamic stability of neutral and negatively charged FeO_n clusters.

(a) Geometries and Electronic Configurations of FeO_n and FeO_n^-, $n = 1-4$. *FeO and FeO*$^-$. Table 1 provides a summary of the results of our calculations for FeO and FeO^-. The ground state of FeO is found to be $^5\Delta$ ($9\sigma^1 4\pi^2 \delta^3$), in agreement with experiment[19,20,66] and previous theoretical[23-27] calculations. As is seen from the table, our computed equilibrium bond length, harmonic frequency, and dipole moment are in good agreement with experiment.[21,66] The states with multiplicities ($M = 2S + 1$) of 3 and 7 are higher in energy by ≈1 eV. Interestingly, even the $M = 9$ state is still thermodynamically stable toward dissociation to the ground-state Fe and O atoms. According to the natural bond analysis (NBO), the natural configurations in the latter state are $Fe(4s^{1.02}3d^{5.64}4p^{1.03})$ and $O(2s^{1.98}2p^{4.29})$; i.e., the 4s electron is promoted to a vacant 4p orbital of Fe. This analysis shows two bonding orbitals for minority-spin electrons: one is of the Fe 4p−O 2p type, and the other one is a hybrid Fe 4s3d−O 2p molecular orbital (MO). Attachment of an extra electron to the ground-state of FeO can result in both high- and low-spin states ($M = 6$ or 4, respectively) of the FeO^- anion. The quartet ($^4\Delta$, $9\sigma^2 4\pi^2 \delta^3$) anionic state is more stable (by 0.2 eV) than the sextet state ($^6\Delta$, $9\sigma^1 10\sigma^1 4\pi^2 1\delta^3$) and corresponds to attachment of an extra electron to the 9σ MO of FeO in agreement with previous assignments.[5,10] Magnetic moments of Fe in the quartet and sextet states of FeO^- differ by 2 μ_B. Since the bond lengths are rather similar, it means that it is energetically easy to increase the magnetic moment of the anion by flipping the spin of a β electron—it costs only about 1600 cm^{-1} or two vibrational quanta.

TABLE 1: Equilibrium Bond Lengths (R_e, Å), Harmonic Vibrational Frequencies (ω_e, cm^{-1}), Total Energies (E_{tot}, Hartrees, Relative to −1338), Magnetic Moments of Atoms (μ_{At}, Bohr Magnetons), and Charges on Atoms (Q_{At}, e), Computed According to the Mulliken Population Analysis Scheme, as Well as Dipole Moments (DM, in Debyes) of FeO and FeO^- Corresponding to the Lowest Energy States for a Given Multiplicity $M = 2S + 1$

FeO					
	$M = 1$	$M = 3$	$M = 5$[a]	$M = 7$	$M = 9$
R_e	1.6126	1.5991	1.6082	1.6910	1.9802
ω_e	894	936	907	800	463
E_{tot}	−0.969 46	−0.982 21	−1.017 41	−0.977 48	−0.760 79
μ_{Fe}	0.74	1.54	3.50	5.00	6.38
μ_O	−0.74	0.46	0.50	1.00	1.62
Q_{Fe}	0.35	0.38	0.40	0.30	−0.08
Q_O	−0.35	−0.38	−0.40	−0.30	0.08
DM	3.40	4.15	4.37	1.86	0.37
FeO^-					
	$M = 2$	$M = 4$[b]	$M = 6$	$M = 8$	$M = 10$
R_e	1.6243	1.6323	1.6850	1.6928	2.0060
ω_e	861	849	792	796	446
E_{tot}	−1.033 07	−1.063 21	−1.055 90	−0.957 94	−0.768 45
μ_{Fe}	1.14	2.66	4.48	5.98	7.53
μ_O	−0.14	0.34	0.52	1.02	1.47
Q_{Fe}	−0.36	−0.33	−0.30	−0.66	−1.04
Q_O	−0.64	−0.67	−0.70	−0.34	0.04
DM	0.71	0.76	0.45	1.31	2.65

[a] Experimental data: $R_e = 1.616$ Å,[20] $\omega_e = 880.6$ cm^{-1},[19] DM = 4.7± 0.2 Debye.[21] [b] Calculational data: $R_e = 1.652$ Å, $\omega_e = 846$ cm^{-1}.[10]

The anionic states with $M = 2$ and 10 are stable with respect to the neutral parent states of corresponding multiplicities but are unstable with regard to low-lying neutral states. These states should be considered as metastable, although they can have appreciable lifetimes since their decay requires flipping spins. The state with $M = 8$ is higher in total energy than the neutral state with $M = 7$. This state seems to correspond to a resonance similar to resonances observed in *sp* systems[67] and could be studied with special DFT-adjusted methods developed within ab initio theories (see, e.g., ref 68). Because the dipole moment of FeO is sufficiently large, the FeO^- anion also possesses dipole-bound states, which have been observed experimentally.[8]

According to the NBO analysis, the atomic configurations in the ground state of FeO are $Fe(s^{0.51}3d^{6.65}4p^{0.07})$ and $O(2s^{1.95}2p^{4.80}3p^{0.01})$. There are one bonding orbital in the α representation (30% Fe 4s3d + 70% O 2s2p) and three bonding MOs in the β representation (the first and the second MOs contain 30% Fe 3d + 70% O 2p and the third MO is again 30% Fe 4s3d + 70% O 2s2p, but the admixture of Fe 4s and O 2s does not exceed 5%).

FeO_2 and FeO_2^-. The results of our computations are summarized in Table 2. We found the ground state of FeO_2 to be $^3B_1$ ($11a_1^1 6b_2^2 4b_1^1 1a_2^2$) followed by two other states, $^3A_1$ ($10a_1^1 11a_1^1 6b_2^2 4b_1^2 1a_2^2$) and $^5B_2$ ($10a_1^1 11a_1^1 6b_2^2 4b_1^1 2a_2^1$), which are above the ground state by 0.03 eV (0.7 kcal/mol) only. All these three states have similar bond lengths, and $^3B_1$ and $^3A_1$ states have similar bond angles. Andrews et al.[31] have found that the $^5B_2$ state is lower than the $^3B_1$ state by 2.4 kcal/mol at the B3LYP level, which is in disagreement with their experimental findings. In a later paper,[32] the authors found the correct ordering of the states when they used the BP86 method. The $^3A_2$ is above the ground $^3B_1$ state by 4.05 eV, and the $^3B_2$ state by 2.63 eV.

TABLE 2: Equilibrium Bond Lengths (R_e, Å), Equilibrium Bond Angles (∠OFeO°, Degrees), Harmonic Vibrational Frequencies (ω, cm^{-1}), Total Energies (E_{tot}, Hartrees, Relative to −1414), Magnetic Moments of Atoms (μ_{At}, Bohr Magnetons), and Charges on Atoms (Q_{At}, e), Computed According to the Mulliken Population Analysis Scheme, as Well as Dipole Moments (DM, Debyes) of FeO_2 and FeO_2^- Corresponding to the Lowest Energy States for a Given Multiplicity $M = 2S + 1$

FeO_2

	$M=1$	$M=3$		$M=5$		$M=7$	$M=9$
	$^1A_1$	$^3B_1$	$^3A_1$	$^5B_2$	$^5A_1$	$^7B_2$	$^9B_1$
R_e	1.5771	1.5867	1.5900	1.6128	1.8284	1.7341	1.8859
∠OFeO	142.5	137.9	142.0	117.1	47.6	120.5	69.7
$\omega(a_1)$	199	197	212	296	425	140	313
$\omega(a_1)$	928	910	899	895	838	719	611
$\omega(b_2)$	1033	1019	1003	932	320	475	358
E_{tot}	−0.258 34	−0.270 77	−0.269 78	−0.268 98	−0.1768 6	−0.208 39	−0.098 35
μ_{Fe}	−0.02	2.08	2.16	3.06	3.18	3.78	5.02
μ_O	0.01	−0.04	−0.08	0.47	0.41	1.11	1.49
Q_{Fe}	0.48	0.52	0.48	0.52	0.46	0.52	0.20
Q_O	−0.28	−0.24	−0.24	−0.26	−0.23	−0.26	−0.10
DM	2.01	2.02	1.72	3.38	5.34	3.56	1.70

FeO_2^-

	$M=2$		$M=4$	$M=6$	$M=8$	$M=10$
	$^2A_2$	$^2B_1$	$^4B_2$	$^6A_1$	$^8B_2$	$^{10}A_1$
R_e	1.8308	1.6228	1.6422	1.7119	1.7953	1.9198
∠OFeO	46.1	148.0	129.8	141.6	90.0	67.4
$\omega(a_1)$	551	177	173	200	218	309
$\omega(a_1)$	913	843	834	751	681	574
$\omega(b_2)$	349	972	890	797	524	371
E_{tot}	−0.209 51	−0.349 84	−0.354 22	−0.341 34	−0.254 58	−0.085 84
μ_{Fe}	1.06	1.24	2.66	3.94	4.78	6.24
μ_O	−0.03	−0.12	0.17	0.53	1.11	1.38
Q_{Fe}	−0.30	0.02	0.15	0.24	−0.10	−0.74
Q_O	−0.35	−0.51	−0.575	−0.62	−0.45	−0.13
DM	0.78	0.03	2.36	2.47	0.63	1.63

Similar to FeO^-, the FeO_2^- anion has three closely spaced states, all of which have their total energies lower than the total energy of the neutral ground state; i.e., these states are stable with respect to autodetachment. The ground state of FeO_2^- is $^4B_2$ ($11a_1^1 6b_2^2 4b_1^1 2a_2^1$) followed by the $^2B_1$ (+0.12 eV, $11a_1^2 6b_2^2 4b_1^1 1a_2^2$) and $^6A_1$ (+0.35 eV, $10_1^1 11a_1^1 7b_2^1 4b_1^1 2a_2^1$) states. Other anionic states displayed in Table 2 are either metastable with respect to detachment of an extra electron or unstable ($M = 10$). Using a CAS-PT2 approach, Schröder et al.[69] have found the ground state of FeO_2^+ to be a quartet as well, which is close in energy to the sextet state. The magnetic moment at Fe is 2 μ_B in the ground state of FeO_2, which means that the magnetic moment is quenched upon attachment of the second oxygen atom to FeO. Interestingly, the two $M = 5$ states with different spatial symmetries of FeO_2 have nearly the same magnetic moments at Fe (see Table 2), although they are separated by an energy gap of 2.5 eV.

The atomic electronic configurations in the ground state of FeO_2 are Fe($4s^{0.38}3d^{6.50}4p^{0.04}$) and O($2s^{1.94}2p^{4.59}3p^{0.01}$). There are two and four bonding MOs in the α and β representations, respectively. The atomic configurations in the ground-state anion are Fe($4s^{0.34}3d^{6.55}4p^{0.11}5s^{0.02}$ $4d^{0.01}5p^{0.01}$) and O($2s^{1.94}2p^{5.00}3s^{0.01}3p^{0.01}$). The anion has one and three bonding MOs in the α and β representations, respectively.

Following the work of Andrews et al.,[31] we have also optimized cyclic (or peroxide, or η^2-complex) Fe(O_2) and superoxide (or η^1-complex) FeOO configurations in addition to the OFeO configuration presented above. The lowest in total energy are states of Fe(O_2) and FeOO with the multiplicity of 5, and they are placed above the OFeO ground state by 2.56 and 2.97 eV, respectively. A detailed report on the structure of OMO, M(O_2), and MOO configurations in the series of 3d-metal dioxides (M = Sc−Zn) will be presented elsewhere.[70]

FeO_3 and FeO_3^-. The results on these clusters are summarized in Table 3. The ground state of FeO_3 is a singlet [$^1A_1'$, $(7a_1')^2(6e_1')^4(3a_2'')^2(1a_2')^2(1e'')^4$] possessing D_{3h} symmetry, which in agreement with previous theoretical results.[32,33] This implies that iron in the ground state of FeO_3 has no unpaired electrons and no permanent magnetic moment can be found in this cluster. The first excited state of FeO_3 with $M = 3$ presents a slightly distorted equilateral triangle of C_{2v} symmetry with the electronic configuration ($13a_1^1 7b_2^2 4b_1^2 2a_2^1$) and is separated from the ground state by 0.37 eV. This energy separation is somewhat larger than the corresponding energy differences between low-lying states in FeO and FeO_2. A subsequent increase in the multiplicity leads to a lowering in symmetry from D_{3h} ($M = 1$) to C_s ($M = 7$). The latter state, which is higher in energy by 3 eV with respect to the ground state, has elongated bond lengths and is still stable toward the dissociation to FeO_2 + O. Optimized structures of different configurations are presented in Figure 1.

Attachment of an extra electron to the ground state of FeO_3 results in the ($^2A_2$, C_{2v}) state of FeO_3^-. Note that the lowest unoccupied MO in the ground state of FeO_3 has e'' symmetry; therefore, spatial symmetry of the doublet anion is reduced due to the Jahn−Teller effect. Attachment of an extra electron into the a_1 MO of the FeO_3 triplet state produces the doublet anion state (C_{2v}, $^2A_2$), whereas attachment to a vacant a_2 MO results in the ($^4A_1'$, D_{3h}) state. Both these anion states have similar geometries and the quartet state is only marginally (by 0.015 eV) lower than the doublet state. Thus, one can surmise that attachment of an additional electron leads to the appearance of a permanent magnetic moment at Fe, which (statistically) equals 1.5 μ_B. The next anion state with $M = 6$, although being well separated from two lowest states, is still stable with respect to autodetachment to the neutral ground state. So, the FeO_3^- anion

TABLE 3: Equilibrium Bond Lengths (R(Fe−O_{ax}) and R(Fe−O_{eq}), Å),[a] Harmonic Vibrational Frequencies (ω, cm^{-1}), Zero-Point Energies (in kcal/mol), Total Energies (E_{tot}, Hartrees, Relative to −1489), Magnetic Moments of Atoms (μ_{At}, in Bohr Magnetons), and Charges on Atoms (Q_{At}, e), Computed According to the Mulliken Population Analysis Scheme, as Well as Dipole Moments (DM, Debyes) of FeO_3 and FeO_3^- Corresponding to the Lowest Energy States for a Given Multiplicity $M = 2S + 1$

FeO_3				
	$M = 1$ D_{3h}, $^1A'_1$	$M = 3$ C_{2v}, $^3A_2$	$M = 5$ C_{3v}, $^5A_2$	$M = 7$ C_s, $^7A''$
R(Fe−O_{ax})	1.5770	1.5878	1.6364	1.6591
R(Fe−O_{eq})	1.5770	1.6041	1.6364	1.7654
	$\omega(a_2'') = 155$	$\omega(b_1) = 111$	$\omega(a_1) = 89$	$\omega(a') = 101$
	$\omega(e') = 329$	$\omega(b_2) = 197$	$\omega(e) = 211$	$\omega(a'') = 137$
	$\omega(e') = 329$	$\omega(a_1) = 343$	$\omega(e) = 211$	$\omega(a') = 210$
	$\omega(a_1') = 915$	$\omega(b_2) = 858$	$\omega(e) = 599$	$\omega(a'') = 505$
	$\omega(e') = 1018$	$\omega(a_1) = 858$	$\omega(e) = 599$	$\omega(a') = 618$
	$\omega(e') = 1018$	$\omega(a_1) = 989$	$\omega(a_1) = 827$	$\omega(a') = 802$
Z	5.38	4.80	3.63	3.39
E_{tot}	−0.515 05	−0.501 25	−0.469 64	−0.404 02
μ_{Fe}	0.0	1.58	1.95	2.79
$\mu_{O_{ax}}$	0.0	−0.28	0.68	0.98
$\mu_{O_{eq}}$	0.0	0.35	0.68	1.11
Q_{Fe}	0.45	0.49	0.44	0.43
$Q_{O_{ax}}$	−0.15	−0.14	−0.15	−0.14
$Q_{O_{eq}}$	−0.15	−0.17	−0.15	−0.15
DM	0.0	0.51	1.16	2.22

FeO_3^-				
	$M = 2$ C_{2v}, $^2A_2$	$M = 4$ D_{3h}, $^4A'_1$	$M = 6$ C_{2v}, $^6A_1$	$M = 8$ C_s, $^8A''$
R(Fe−O_{ax})	1.6037	1.6423	1.6887	1.8387
R(Fe−O_{eq})	1.6258	1.6423	1.7306	1.8218
	$\omega(b_2) = 191$	$\omega(b_1) = 176$	$\omega(b_2) = 109$	$\omega(a'') = 101$
	$\omega(b_1) = 252$	$\omega(b_2) = 307$	$\omega(b_1) = 137$	$\omega(a') = 119$
	$\omega(a_1) = 333$	$\omega(a_1) = 308$	$\omega(a_1) = 218$	$\omega(a') = 133$
	$\omega(b_2) = 805$	$\omega(a_1) = 806$	$\omega(b_2) = 677$	$\omega(a'') = 480$
	$\omega(a_1) = 846$	$\omega(b_2) = 899$	$\omega(a_1) = 720$	$\omega(a') = 486$
	$\omega(a_1) = 961$	$\omega(a_1) = 900$	$\omega(a_1) = 795$	$\omega(a') = 609$
Z	4.85	4.86	3.80	2.76
E_{tot}	−0.636 56	−0.635 96	−0.570 76	−0.490 59
μ_{Fe}	0.68	2.24	2.92	3.79
$\mu_{O_{ax}}$	−0.14	0.25	0.43	1.21
$\mu_{O_{eq}}$	0.23	0.25	0.82	1.00
Q_{Fe}	0.34	0.41	0.34	0.33
$Q_{O_{ax}}$	−0.43	−0.47	−0.55	−0.41
$Q_{O_{eq}}$	−0.45	−0.47	−0.39	−0.46
DM	0.61	0.0	0.03	2.13

[a] The subscripts "ax" and "eq" designate one nonequivalent and two equivalent oxygen atoms, respectively; $\mu_{O_{eq}}$ is the sum of magnetic moments on two equivalent oxygen atoms.

has at least three states stable toward autodetachment of the extra electron. The anion state with $M = 8$ is well below its neutral parent $M = 7$ state and could, probably, exist as a metastable state.

It is worth noting that the geometric configurations of both FeO_3 and FeO_3^- presented in Figure 1 are either planar or nearly planar. For ordinary *sp* compounds it is not so: spin excitations result generally in dramatic changes in geometry, which usually are described in terms of *sp* hybridization. Also, attachment of an extra electron leads typically to rather appreciable changes in the geometry of a neutral *sp* parent. On the contrary, attachment of an extra electron does not lead to a considerable change of either bond lengths or bond angles in iron oxides.

According to the NBO analysis, iron has a ($4s^{0.37}3d^{6.62}4p^{0.02}$) configuration and each oxygen has a ($2s^{1.92}2p^{4.39}$) configuration in the ground state of FeO_3, and there are seven bonding orbitals (plus six lone pairs). Attachment of an extra electron results in

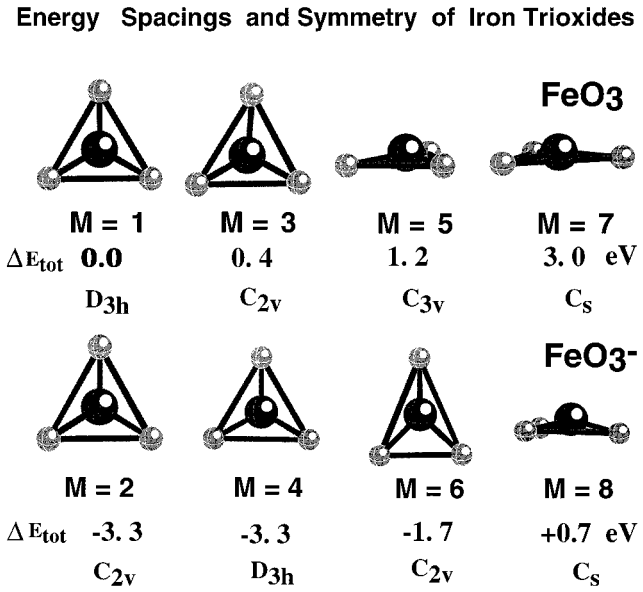

Figure 1. Geometrical configurations of the ground and excited states of FeO_3 and FeO_3^-. Bond angles $\angle O_{ax}FeO_{eq}$ and $\angle O_{eq}FeO_{eq}$ (in degrees) between equivalent pairs of oxygen atoms are as follows. FeO_3: 120.0 and 120.0 ($M = 1$); 123.0 and 113.9 ($M = 3$); 118.0 and 118.0 ($M = 5$); 96.4 and 159.8 ($M = 7$); FeO_3^-: 122.7 and 114.6 ($M = 2$);120.0 and 120.0 ($M = 4$); 135.1 and 89.8 ($M = 6$); 98.7 and 149.5 ($M = 8$).

the following electronic configurations of the FeO_3^- anion: Fe($4s^{0.40}3d^{6.65}4p^{0.02}$), $O_{1,2}$($2s^{1.93}2p^{4.73}$), and O_3($2s^{1.93}2p^{4.67}$). The anion has seven bonding orbitals and seven lone pairs in the α configuration and nine bonding orbitals and four lone pairs in the β configuration. Thus, the extra electron is delocalized over oxygens, which results in a relatively high A_{ad} of FeO_3 (about 3.3 eV). Attachment of an extra electron transforms a lone pair of FeO_3 into two bonding orbitals in FeO_3^-, which results in a higher thermodynamic stability of the latter.

FeO_4 and FeO_4^-. The results on these clusters are given in Table 4, and geometrical configurations are displayed in Figure 2. Iron in FeO_4 has fully saturated its formal valence ($k = 8$), and the ground state of FeO_4 is expected to be totally symmetric. Indeed, according to the results of our computations, its equilibrium configuration has T_d symmetry ($^1A_1$, $6a_1^2 6t_2^6 1e^4 1t_1^6$), which is in contradiction with the result of Chertihin et al.[32] who predicted a configuration $(O_2)FeO_2$ with C_{2v} symmetry to be the lowest in energy. This configuration is followed by a configuration of T_d symmetry that lies 7.5 kcal/mol higher. On the contrary, we found the $(O_2)FeO_2$ configuration ($^1A_1$, $14a_1^2$-$7b_2^2 6b_1^2 2a_2^2$) denoted in Table 4 as (C_{2v}, $^1A_1$) to be higher in energy by 4.7 kcal/mol with respect to the T_d configuration.

There are no experimental data on the gas-phase geometry of FeO_4; however, isoelectronic RuO_4 and OsO_4 are experimentally found to have T_d symmetry.[72] Taking this into account and keeping in mind that our computations are performed with a somewhat better *spdf* basis than that used by Chertihin et al.,[32] we expect the ground state of the gas-phase FeO_4 cluster to possess a T_d configuration. Experimental confirmation of our prediction is eagerly awaited.

To understand the internal structure of these two closely spaced isomers of FeO_4, we discuss in the following the results of our NBO analysis for both T_d and C_{2v} singlet states of FeO_4. The electronic configurations of atoms in FeO_4 are as follows: T_d Fe($4s^{0.27}3d^{6.68}4p^{0.02}4f^{0.01}5d^{0.01}$) and O($2s^{1.93}2p^{4.32}$), and there are eleven bonding orbitals and five lone pairs; C_{2v} Fe($4s^{0.29}$-$3d^{6.66}5p^{0.02}$), $O_{1,2}$($2s^{1.92}2p^{4.39}$), and $O_{3,4}$($2s^{1.86}2p^{4.30}$), where $O_{1,2}$ refers to oxygens with shorter bond lengths and a larger bond

TABLE 4: Equilibrium Bond Lengths, Harmonic Vibrational Frequencies, Magnetic Moments of Atoms, and Dipole Moments of FeO_4 FeO_4^- for Different Multiplicities $M = 2S + 1$[a]

FeO_4

	M = 1		$M = 3$	$M = 5$	$M = 7$
	(T_d, $^1A_1$)	(C_{2v}, $^1A_1$)	(C_{2v}, $^3B_1$)	(C_{2v}, $^5B_1$)	(D_{2d}, $^7A_2$)
$R_{1,2}$	1.5961	1.5691	1.5843	1.6172	1.7095
$R_{3,4}$	1.5961	1.7805	1.6714	1.6974	1.7095
	$\omega(e) = 361$	$\omega(b_2) = 255$	$\omega(a_1) = 271$	$\omega(b_1) = 89$	$\omega(e) = 77$
	$\omega(e) = 361$	$\omega(b_1) = 259$	$\omega(a_2) = 284$	$\omega(a_1) = 153$	$\omega(e) = 77$
	$\omega(t_2) = 412$	$\omega(a_2) = 317$	$\omega(b_1) = 317$	$\omega(b_2) = 157$	$\omega(b_1) = 168$
	$\omega(t_2) = 412$	$\omega(a_1) = 320$	$\omega(b_2) = 343$	$\omega(a_2) = 191$	$\omega(a_1) = 248$
	$\omega(t_2) = 412$	$\omega(b_1) = 577$	$\omega(a_1) = 363$	$\omega(a_1) = 320$	$\omega(b_2) = 273$
	$\omega(a_1) = 881$	$\omega(a_1) = 592$	$\omega(b_1) = 692$	$\omega(b_1) = 656$	$\omega(e) = 537$
	$\omega(t_2) = 955$	$\omega(a_1) = 972$	$\omega(a_1) = 807$	$\omega(b_2) = 684$	$\omega(e) = 537$
	$\omega(t_2) = 955$	$\omega(a_1) = 1005$	$\omega(a_1) = 945$	$\omega(a_1) = 739$	$\omega(b_2) = 732$
	$\omega(t_2) = 955$	$\omega(b_2) = 1018$	$\omega(b_2) = 984$	$\omega(a_1) = 832$	$\omega(a_1) = 738$
Z	8.15	7.60	7.16	5.46	4.84
E_{tot}	−0.710 65	−0.703 08	−0.681 37	−0.647 87	−0.601 57
μ_{Fe}	0.0	0.0	0.43	0.84	1.66
$\mu_{O_{1,2}}$	0.0	0.0	−0.06	0.48	1.085
$\mu_{O_{3,4}}$	0.0	0.0	0.84	1.10	1.085
Q_{Fe}	0.15	0.39	0.15	0.12	0.18
$Q_{O_{1,2}}$	−0.04	−0.17	−0.07	−0.08	−0.045
$Q_{O_{3,4}}$	−0.04	−0.03	−0.0	0.025	−0.045
DM	0.0	0.0	0.28	0.24	0.0

FeO_4^-

	$M = 2$		$M = 4$	$M = 6$	$M = 8$
	(D_{2d}, $^2A_1$)	(C_{2v}, $^2A_2$)	(C_{2v}, $^4B_2$)	(D_{2d}, $^6B_2$)	(D_{2h}, $^8A_2$)
$R_{1,2}$	1.6312[b]	1.6121	1.6276	1.7134	1.7833
$R_{3,4}$	1.6312	1.8132	1.6983	1.7134	1.7833
	$\omega(a_1) = 314$	$\omega(b_2) = 219$	$\omega(a_1) = 230$	$\omega(a_2) = 160$	$\omega(b_2) = 113$
	$\omega(b_2) = 317$	$\omega(b_1) = 223$	$\omega(a_2) = 242$	$\omega(b_1) = 167$	$\omega(a_1) = 153$
	$\omega(b_1) = 364$	$\omega(a_2) = 235$	$\omega(b_1) = 250$	$\omega(b_2) = 167$	$\omega(b_1) = 182$
	$\omega(e) = 378$	$\omega(a_1) = 318$	$\omega(b_2) = 272$	$\omega(a_1) = 266$	$\omega(a_1) = 235$
	$\omega(e) = 378$	$\omega(b_2) = 418$	$\omega(a_1) = 347$	$\omega(a_1) = 314$	$\omega(a_1) = 290$
	$\omega(a_1) = 825$	$\omega(a_1) = 576$	$\omega(b_1) = 620$	$\omega(b_1) = 546$	$\omega(b_2) = 595$
	$\omega(b_2) = 848$	$\omega(a_1) = 891$	$\omega(a_1) = 768$	$\omega(b_2) = 547$	$\omega(a_1) = 601$
	$\omega(e) = 880$	$\omega(b_2) = 908$	$\omega(b_2) = 830$	$\omega(a_1) = 728$	$\omega(b_2) = 604$
	$\omega(e) = 880$	$\omega(a_1) = 925$	$\omega(a_1) = 862$	$\omega(a_1) = 824$	$\omega(a_1) = 660$
Z	7.41	6.74	6.32	5.32	4.91
E_{tot}	−0.84886	−0.814546	−0.82299	−0.77231	−0.72115
μ_{Fe}	0.55	0.65	1.01	1.80	2.82
$\mu_{O_{1,2}}$	0.11	0.17	0.26	0.80	1.04
$\mu_{O_{3,4}}$	0.11	0.01	0.735	0.80	1.04
Q_{Fe}	0.20	0.36	0.20	0.22	0.33
$Q_{O_{1,2}}$	−0.30	−0.435	−0.34	−0.305	−0.33
$Q_{O_{3,4}}$	−0.30	−0.245	−0.26	−0.305	−0.33
DM	0.00	0.54	0.18	0.0	0.0

[a] Bond lengths [R(Fe−O_i)] are in Å, harmonic vibrational frequencies (ω) are in cm^{-1}, zero-point vibrational energies (Z) are in kcal/mol, total energies (E_{tot}, relative to −1564) are in hartrees, magnetic moments μ_{At} are in Bohr magnetons, and charges on atoms (Q_{At}, in e), computed according to the Mulliken population analysis scheme, as well as dipole moments (in Debyes). [b] The experimental Fe−O bond length measured for a $[FeO_4]^{2-}$ unit in salts is 1.650 ± 0.010 (see ref 71).

angle. In the latter case, one sees an increase in the donation of O 2s into the bonding due to a shorter O−O distance. This C_{2v} isomer has 10 bonding orbitals and five lone pairs; i.e., formally, it is less preferable with respect to the T_d isomer, whose structure seems to provide a better opportunity for bonding. It is worth mentioning that although the iron atomic configurations are nearly the same in both cases, the individual 3d atomic orbitals have different populations. In the T_d case, 3d populations are the following: $3d_{xy}^{1.40}$ $3d_{z^2}^{1.40}$ $3d_{xz}^{1.29}$ $3d_{yz}^{1.29}$ $3d_{x^2-y^2}^{1.29}$ (a classic example of e−t_2 splitting of an atomic d manifold by a T_d crystalline field), whereas in the C_{2v} case, they are $3d_{xy}^{1.25}$ $3d_{z^2}^{1.55}$ $3d_{xz}^{1.14}$ $3d_{yz}^{1.16}$ $3d_{x^2-y^2}^{1.56}$. Another view is to consider the C_{2v} isomer as "FeO_3", where one oxygen is replaced by a single-bonded molecular dioxygen.

According to our calculations, the triplet state of FeO_4 has C_{2v} symmetry and is separated from the ground state by 0.8 eV. In this state, the magnetic moments of oxygen atoms are localized at the sites forming a longer bond (see Table 4). This could indicate that the latter oxygens behave as monovalent ligands, having one unpaired electron each. Let us recall that the ground state of the oxygen molecule is a triplet ($^3\Sigma_g^-$). Further excitations up to $M = 7$ lead to equalizing all bond distances in D_{2d} symmetry, where all oxygen atoms have the same formal valence, $k = 1$.

The lowest unoccupied MO of FeO_4 in its ground state has E symmetry and filling of an extra electron into this MO should lead to a Jahn−Teller distortion of the resulting anion. Indeed, the ground state of FeO_4^- is a doublet of D_{2d} symmetry ($^2A_1$, $8a_1^1 6e^4 7b_2^2 2b_1^2 1a_2^1$) and its geometry represents a slightly distorted tetrahedron. The optimized bond length of 1.631 Å is close to the value of 1.650 ± 0.010 obtained in an X-ray study of salts formed by organic ligands and $[FeO_4^{2-}]$.[71] The

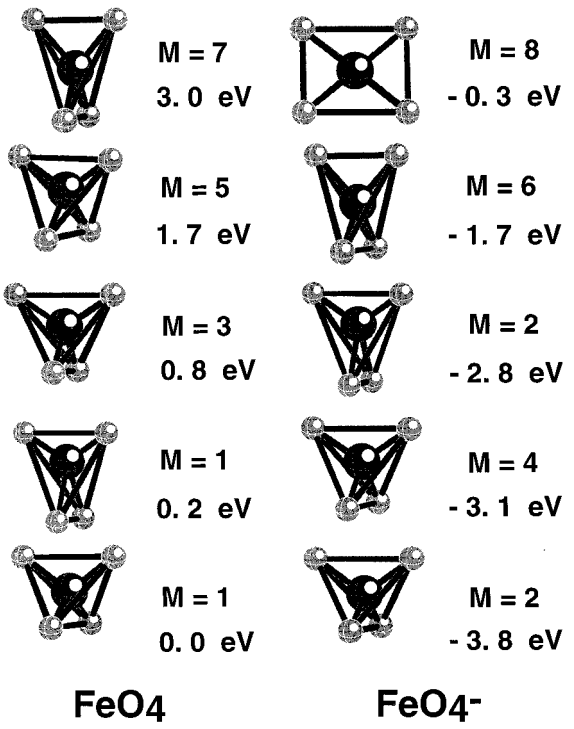

Figure 2. Geometrical configurations of the ground and excited states of FeO_4 and FeO_4^-. Bond angles (in degrees) between equivalent pairs of oxygen atoms are as follows. FeO_4: 109.47 ($M = 1$, T_d); 119.1 and 45.8 ($M = 1$, C_{2v}) 115.9 and 88.5 ($M = 3$); 116.2 and 88.7 ($M = 5$); 81.7 and 81.7 ($M = 7$). FeO_4^-. 110.0 ($M = 2$, D_{2d}); 116.2 and 47.2 ($M = 2$); 113.7 and 91.1 ($M = 4$); 86.0 and 86.0 ($M = 6$); 103.0 and 103.0 ($M = 8$, D_{2d}).

anion has the second doublet state of C_{2v} symmetry ($^2A_2$, $14a_1^2 7b_2^2 6b_1^2 3a_2^1$), whose geometry is similar to that of the ($^1A_1$, C_{2v}) neutral state (see Table 4 and Figure 2). The $^2A_2$ state is separated from the ground anion state by 0.93 eV (21.5 kcal/mol), i.e., the anion appears to be more rigid than its neutral parent, and we will see below that the FeO_4^- anion is thermodynamically more stable than FeO_4. According to the NBO analysis, the ground-state anion has seven bonding orbitals and ten lone pairs in the α representation and ten bonding orbitals and six lone pairs in the β representation. Its C_{2v} isomer is less bound, having five bonding orbitals and twelve lone pairs in the α representation and six bonding orbitals and ten lone pairs in the β representation. In the ground-state anion, the atomic configurations are $Fe(4s^{0.25}3d^{6.60}4p^{0.02}4d^{0.02})$ and $O(2s^{1.93}2p^{4.59})$; i.e., the additional electron is delocalized over four oxygen atoms. More specifically, the highest occupied MO of FeO_4^- is a linear combination $d_{xy}(Fe) + p_x(O_1,O_3) - p_x(O_2,O_4)$ and is of a bonding type with respect to oxygen−oxygen interaction and is slightly antibonding with respect to Fe−O interactions because the contribution of Fe 3d orbitals is about 10% only.

Keeping in mind that FeO_4 represents a closed-shell system with fully saturated formal valences, one could anticipate, by analogy with *sp* compounds, that attachment of an additional electron to FeO_4 will lead to a weakly bound anion. Surprisingly, the FeO_4^- anion is not only rather stable with respect to its ground-state parent but also possesses several excited states, all of which are stable with respect to autodetachment. Even the exited state with $M = 8$, whose configuration can be described as $[Fe(O_2)_2]^-$, is still bound by 0.3 eV compared to the neutral ground state. Actually, two different types of $[FeO_4^-][Na^+]$ centers have been observed in a silica glass.[73]

(b) Charges and Spin Distributions. To achieve a qualitative understanding of charge and spin distributions in various iron oxide clusters as a function of their spin multiplicity, let us consider the magnitudes of charges on atoms and local spin moments at atomic sites evaluated according to the Mulliken population analysis scheme. As can be seen from Tables 1−4, the charges on Fe atoms are about the same and practically independent of their spin multiplicities, except for states with the highest multiplicities, in all neutral FeO_n clusters.

There is a charge transfer from Fe to O atoms. Since the net charge on the Fe sites is insensitive to the oxygen decoration, the net charge on each oxygen is reduced in higher oxides, approaching zero value in FeO_4. Thus, the coupling in FeO could be interpreted as having a more ionic character while in larger oxide clusters these become more covalent. The relative strength in bonding diminishes as more oxygen atoms are added to Fe. In anionic clusters, the extra electron is shared mainly by the oxygen atoms (except for FeO^-), thus making FeO_n^- clusters more thermodynamically stable than neutral FeO_n for $n = 2-4$.

The magnetic coupling between Fe and oxygen atoms in FeO_n clusters can be examined by considering the spin moments at each atomic site. These are calculated using the Mulliken analysis in the same way the charges are calculated except that here one integrates the difference between spin densities $\rho(r) = \rho^\alpha(r) - \rho^\beta(r)$ after separating it into partial atomic contributions.

One can see from Tables 1−4 that only low-spin multiplicity states of iron oxides exhibit antiferromagnetic coupling. As multiplicity increases, the coupling becomes ferromagnetic with magnetic moments at O sites approching 1 μ_B or even higher in the highest multiplicity states. Such a behavior of magnetic moments on oxygens can be related with the necessity for the central atom, Fe, to share some of its valence electrons with oxygens in order to form chemical bonds. So, unpaired electrons cannot be localized entirely at the central atom and are distributed over ligand atoms as well.

This can also can be viewed in another way. The virtual orbitals in the iron oxide ground states are mainly oxygen-based, and flipping an electron results in the occupation of an oxygen-based molecular spin−orbital. The latter leads to an increase in the number of α electrons with respect to the number of β electrons on oxygens and, consequently, to an increase in the magnetic moments on oxygens.

(c) Vibrational Frequencies. Andrews et al.[31,32] have obtained infrared spectra of products resulting from reactions of laser-ablated Fe atoms with oxygen molecules in condensing argon. Their assignment of experimental features was based on considerations of oxygen isotopic shifts and multiplets in matrix infrared spectra supplemented with DFT-based calculations. Here, we would like to compare their assignment with the results of our frequency calculations. Note, that the theory produces harmonic frequencies that are generally larger than experimental fundamental frequencies because anharmonic corrections are negative.[74]

OFeO. Two sharp bands at 945 and 797 cm^{-1}, which should correspond to the b_2 antisymmetric mode active in infrared spectra, were attributed to the bent OFeO molecule.[32] As seen from Table 2, the peak at 945 cm^{-1} could correspond to the FeO_2 ground state [$\omega(b_2) = 1003$ cm^{-1}]. At the same time, one can attribute this peak to the $^2B_1$ state of the anion [$\omega(b_2) = 972$ cm^{-1}] and the peak at 797 cm^{-1} to the $^6A_1$ state of the anion [$\omega(b_2) = 797$ cm^{-1}]. The presence of several closely spaced states in both neutral and negatively charged species with unknown concentrations together with the lack of informa-

tion on symmetric stretching modes makes precise assignment of experimental findings rather difficult.

FeO_3. Andrews et al.[31] assigned the 975.8 cm^{-1} band to the antisymmetric stretching fundamental of the ground state FeO_3 species. Our computed frequency for the ground-state of FeO_3 $\omega(e') = 1018$ cm^{-1} is in reasonable agreement with this experiment.

FeO_4. The experimental assignment of bands for singlet and triplet states of FeO_4 was based on results of calculations performed in the same work.[31] Assignment of the 968.9 cm^{-1} band to the $(O_2)FeO_2$ isomer, corresponding to the (C_{2v},$^1A_1$) configuration in Table 4 does not contradict our results, since the most intense mode $\omega(b_2)$ is at 1008 cm^{-1}. No assignment for the tetrahedral configuration has been done in ref 31. Note that the attachment of an extra electron leads to the decrease in the magnitudes of the frequencies of FeO_4^- anion, which are getting close to experimental fundamentals measured for $[FeO_4]^{2-}$ units in salts,[75] namely, $\nu(E) = 322$, $\nu(T_2) = 340$, $\nu(A_1) = 790$, $\nu(T_2) = 832$ cm^{-1}.

(d) Electron Affinities. The adiabatic electron affinity (A_{ad}) of a neutral molecular system is defined as the difference in the ground-state total energies of the system and its anion. Within the Born−Oppenheimer approximation employed in the present work, one may evaluate the A_{ad} as

$$A_{ad} = E_{tot}(N,R_e) + Z_N - E_{tot}(A,R_e^-) - Z_A = \Delta E_{el}^{ad} + \Delta E_{nuc} \quad (4)$$

where R_e and R_e^- denote equilibrium bond lengths of a neutral molecule (N) and its anion (A), respectively. The zero-point vibration energies (Z) are computed usually within the harmonic approximation.

Another useful quantity that characterizes a "sudden" detachment of an extra electron from an anion, i.e., when clusters had not enough time to relax after removal of the extra electron, is the so-called vertical detachment energy (E_{vd}). The E_{vd} can be calculated as

$$E_{vd} = E_{tot}(N,R_e^-) - E_{tot}(A,R_e^-) \quad (5)$$

In many cases, the E_{vd} corresponds to a feature with the maximum (or near-maximum) intensity in the corresponding envelope of a photoelectron spectrum.[76] Comparing the computed A_{ad} and E_{vd} for a particular anion−neutral pair allows one to evaluate "nonadiabatic" corrections[77] related to the difference between equilibrium geometries of an anion and its neutral parent. If such corrections are large, the origin of the photodetached electron envelope cannot be resolved accurately because corresponding features will have small intensities (of the same order of magnitude as the background) due to vanishingly small Franck−Condon factors. This is definitely the case for such molecules as CS_2 or SF_6. In the first case, the experimental photoelectron spectrum "disappears" at about 0.8 eV, whereas the A_{ad} of CS_2 is computed to be 0.3 eV.[78] This "discrepancy" is related to large changes in the geometry of CS_2 (from linear to angular) upon attachment of an extra electron. In the second case, the attachment of an extra electron leads to a rather large increase in the bond length without changing the octahedral symmetry. Again, Franck−Condon factors for the 0−0 transitions appears to be too small and the peak with highest intensity is observed at about 3.2 eV, whereas the A_{ad} is about 1.0 eV.[79]

Adiabatic electron affinities of the neutral FeO_n series and the vertical detachment energies of the corresponding anions have been calculated according to eqs 4 and 5, respectively. The results are compared with experimental data in Table 5. We have also calculated electron affinities of O, Fe, and O_2, since there are available experimental data.[80,81] With the exception of the Fe atom, our results agree well with experiment (note that the experimental value for O_2 corresponds to the adiabatic electron affinity). The poor agreement in the case of the Fe atom is easily understandable, as one needs to use sufficiently diffuse basis functions, which are lacking in the standard 6-311+G* basis set for Fe, to describe loosely bound electrons. This becomes a less severe problem in clusters as bonding makes electrons less diffuse. The A_{ad} of FeO has been measured by two experimental groups,[5−7] and our value is somewhat underestimated compared to experiment (by 0.23 eV). As one can notice from Table 5, the adiabatic corrections, defined as the differences between the A_{ad}'s and E_{vd}'s of each FeO_n−FeO_n^- pair, are rather small, which is indicative that attachment of an extra electron does not lead to significant changes in the geometry of neutral ground-state parents. This is unlike the situation in the majority of the *sp* clusters, where attachment of an extra electron, especially to closed-shell species, results in considerable geometric changes. In many cases, *sp* anions have geometrical shapes different from those of their neutral parents.[63,82,83]

Experimental A_{ad} estimates[5,6] for FeO_2 and FeO_3 are within 0.1 eV from our values, whereas a discrepancy of 0.5 eV is observed for FeO_4 (see Table 5). On the basis of previous results, we expect the accuracy of our calculations not to be worse than 0.1−0.2 eV; therefore, such a discrepancy appears to indicate that either an electron is detached from some excited anion state or from an isomer of the ground-state FeO_4^- anion. As a matter of fact, the A_{ad} of FeO_4 with respect to the ($^2A_2$, C_{2v}) anion state is 3.07 eV and the vertical attachment energy from this anion isomer is 3.24 eV, which corresponds to the location of the first low-energy peak in photodetachment spectra of Wang et al.[6] Figure 3 presents a schematic picture of the energies needed for detachment from the ground-state anion and its isomer.

TABLE 5: Adiabatic Electron Affinities (A_{ad}) of Neutral Species and Vertical Detachment Energies E_{vd}) of the Corresponding Anions Calculated According to eqs 4 and 5[a]

	O	Fe	O_2	FeO	FeO_2	FeO_3	FeO_4
A_{ad}	1.63	0.61	0.47	1.26	2.29	3.34	3.79
E_{vd}	1.63	0.61	0.96	1.29	2.52	3.47	3.90
exp[b]	1.46	0.16	0.44	1.49	2.36	3.26	3.30

[a] All values are in eV. [b] Experimental values for atoms are from ref 80; for O_2 are from ref 81: for FeO are from ref 7; for FeO_2, FeO_3, and FeO_4 are from ref 6.

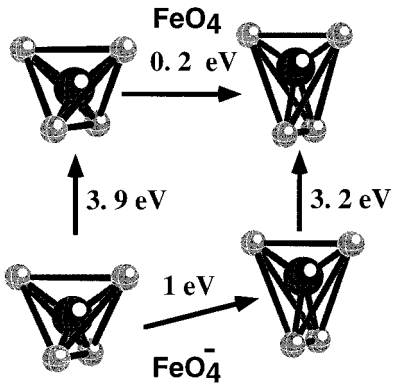

Figure 3. Scheme of detachment of an extra electron from two states of FeO_4^-.

TABLE 6: Energies of Vertical Electron Detachment from Low-Lying FeO_4^- States (See Text)[a]

FeO_4^-			FeO_4 $2S+1$		
$2S+1$	symm	ΔE_{tot}	1	3	5
2	D_{2d}	0.0	3.9	4.9	
	C_{2v}	0.9	3.2	4.2	
	TS B_1, B_2	1.4	2.8	3.8	
4	C_{2v}	0.7		4.9	4.9

[a] All values are in eV.

To check if additional anion states may be responsible for the appearance of low-energy features in the photodetachment spectra, we have optimized the anion geometry within C_{2v} constraints for all four types of irreducible representations of this point-group symmetry starting with the $^2A_2$ geometrical parameters. The geometry and total energy of the $^2A_1$ state have converged to the ground-state geometry and the total energy, respectively, whereas $^2B_1$ and $^2B_2$ states were found to have the same geometrical parameters which are close to those of the neutral $M = 3$ state and are energetically degenerate. Frequency calculations have yielded one imaginary mode of the a_2 symmetry, which couples these two transition states ($B_1 * a_2 * B_2 = A_1$). Coupling through a mode of corresponding symmetry can lead to a transition into the ground or C_{2v} stationary states.

Summary of our calculations of the vertical detachment energies of different states of FeO_4^- are presented in Table 6. As is seen, detachment of an extra electron from the isomer ($M = 2$, C_{2v}) anion state could explain the appearance of low-energy features at 3.2−3.3 eV, which have essentially lower intensities than the features around ≈4.0 eV in the photodetachment spectra obtained by Wang et al.[6] This isomer, which could be produced by vibrational excitations of the ground-state anion (in case it is not already present in the initial anion flow), should have a relatively large lifetime, since the computed barrier to its interconversion to the ground state is ≈0.6 eV.

The A_{ad} of FeO_3 is close to the EA of F atom (3.40 eV) and the A_{ad} of FeO_4 exceeds the EA of Cl (3.62 eV), the most electronegative atom in the Periodic Table.[80] Thus, FeO_4 can be attributed to the class of superhalogens[77] despite its closed-shell structure. This is in sharp contrast with *sp* compounds, where superhalogens of the MO_m type (e.g., AlO_2, PO_3, ClO_4) do satisfy the relation $2m = k + 1$, where k is the maximum formal valence of the central atom M, and an extra electron fills in the MO, which does not contain contributions from the central atom by symmetry.[84]

(e) Thermodynamic Stability. The thermodynamic stability of clusters can be studied by analyzing their fragmentation energies that correspond to the differences in total energies between the parent and clusters formed in a particular decay channel, namely,

$$D_0(M) = \sum_i [E_{tot}(F_i) + Z_{F_i}] - E_{tot}(M) - Z_M = D_e(M) + \Delta Z_{nuc} \quad (6)$$

The zero-point energies, Z, are calculated, as before, by using the harmonic approximation. For iron oxides considered in the present work, major fragmentation channels involve O, O_2, or their anions as products.

Energetics of various fragmentation channels of both FeO_4 and FeO_4^- series are calculated according to eq 6, which includes the energy of nuclear motions determined in the harmonic approximation. The results are presented in Table 7

TABLE 7: Fragmentation Energies [$D_0(D_e)$, eV] of FeO_n and FeO_n^-, Computed According to Eq 6

FeO_4		FeO_4^-	
channel	D_0 (D_e)	channel	D_0 (D_e)
$O_2 \rightarrow 2O$	5.83 (5.72)	$O_2^- \rightarrow O + O^-$	4.64 (4.57)
$FeO \rightarrow Fe + O$	5.32 (5.22)	$FeO^- \rightarrow Fe + O^-$	4.94 (4.89)
		$\rightarrow Fe^- + O$	5.96 (5.91)
$FeO_2 \rightarrow Fe + O_2$	4.30 (4.27)	$FeO_2^- \rightarrow FeO + O^-$	5.44 (5.39)
$\rightarrow FeO + O$	4.80 (4.73)	$\rightarrow FeO^- + O$	5.83 (5.78)
		$\rightarrow Fe^- + O_2$	5.96 (5.95)
		$\rightarrow Fe + O_2^-$	6.13 (6.09)
$FeO_3 \rightarrow FeO + O_2$	3.53 (3.47)	$FeO_3^- \rightarrow FeO^- + O_2$	5.59 (5.44)
$\rightarrow FeO_2 + O$	4.56 (4.46)	$\rightarrow FeO_2^- + O$	5.60 (5.50)
		$\rightarrow FeO_2 + O^-$	6.23 (6.16)
		$\rightarrow FeO + O_2^-$	6.40 (6.33)
$FeO_4 \rightarrow FeO_2 + O_2$	1.96 (1.74)	$FeO_4^- \rightarrow FeO_2^- + O_2$	3.45 (3.34)
$\rightarrow FeO_3 + O$	3.23 (3.11)	$\rightarrow FeO_3^- + O$	3.68 (3.56)
		$\rightarrow FeO_2 + O_2^-$	5.28 (5.16)
		$\rightarrow FeO_3 + O^-$	5.36 (5.27)

[a] Experimental bond rupture energies are 5.12 and 4.1 eV for O_2 and O_2^-, respectively,[66] and 4.03 ± 0.13 eV for FeO.[18]

and compared with the only available experiment on FeO,[18] O_2, and O_2^-.[66] Our theoretical values are overestimated by ≈0.5 eV (11.5 kcal/mol) for O_2 and O_2^- and by 1 eV for FeO. Although larger basis sets (and better exchange-correlation functionals) seem to be required for quantitative agreement, we believe that our results reproduce qualitative trends in both series rather correctly.

We note two novel results from Table 7. First, the lowest dissociation channel corresponds to the abstraction of a O_2 dimer but not an oxygen atom, as is usually the case for *sp* compounds and titanium,[85] vanadium,[86] or chromium[87] oxides. The only exception is noted for FeO_2^- where the lowest dissociation channel corresponds to the loss of O^-. This is because the difference in the EAs of Fe and O is larger than the difference in the bond rupture energies in FeO and O_2. Second, the anions FeO_2^-, FeO_3^-, and FeO_4^- are thermodynamically more stable than their neutral precursors. FeO_3^- is the most stable cluster against fragmentation among this series.

In the neutral clusters, we can see a gradual decrease in bond rupture energies with increasing n. The difference between the energies of decay channels with evolution of O_2 and O increases from FeO to FeO_4. The same trends do not hold for the anion series, which is lacking a gradual decrease in the dissociation energies with the increase in n, and energy differences between two uppermost decay channels to O_2 and O are rather small.

The higher thermodynamic stability of FeO_3^- and FeO_4^- with respect to their closed-shell neutral parents is again in contradiction with the usual trends in *sp* compounds, where, usually, only closed-shell anions are more stable than their parent radicals. In the case of *sp* superhalogens, the neutral MX_{k+1} systems are either barely stable (LiF_2, $LiCl_2$, NaF_2, and $NaCl_2$,[88] BF_4 and AlF_4[89]) or even dissociative (PF_6[90,91]), but the anions are very stable against the emission of F^-.

Summary

Our self-consistent calculations of the electronic and geometrical structure of FeO_n and FeO_n^- series (n=1−4) reveal many interesting features. First, iron oxides with lower coordination numbers possess several stationary states that are very close in energy to their corresponding ground states. This means that a change in magnetization (i.e., spin realignment) in the clusters is easy to achieve. The ground-state multiplicity of these clusters decreases gradually from 5 in FeO to 3 in FeO_2 and to

1 in FeO_3. Additional oxygen decoration (i.e., in FeO_4) has no further effect.

Our calculated values of the adiabatic electron affinities (A_{ad}) of FeO_n are in good agreement with recent experimental data. This suggests that density-functional theory at the BPW91 level can quantitatively account for the properties of transition metal oxides. It is found that the A_{ad} of the closed-shell FeO_4 cluster exceeds the electron affinity of the most electronegative atoms Cl. Thus, FeO_4 presents a new type of superhalogen.

The preferred dissociation channels (i.e., channels requiring the least energy for fragmentation) in FeO_2, FeO_3, FeO_4, FeO_3^-, and FeO_4^- correspond to abstraction of the O_2 dimer rather than a rupture of an Fe−O bond. Surprisingly, the FeO_3^- and FeO_4^- anions are more thermodynamically stable than their neutral parents. This is in a sharp contrast to what is known for a majority of *sp* clusters.

Acknowledgment. This work was supported in part by a grant from Department of Energy (DE-FG05-96ER45579). We greatly appreciate stimulating discussions with Professors R. J. Bartlett, H. B. Schlegel, N. Rösch, S. B. Trickey, and L. S. Wang. We thank Dr. V. G. Zakrzewski for the help in a more effective use of GAUSSIAN94.

References and Notes

(1) Baibich, M. N.; Broto, J. M.; Fert, A.; Dau, F. N. V.; Petroff, F. *Phys. Rev. Lett.* **1988**, *61*, 2472.
(2) Parkin, S. S. P.; Marks, R. F.; Farrow, R. F. C.; Harp, G. R.; Lam, Q. H.; Savoy, R. J. *Phys. Rev. B* **1992**, *46*, 9262.
(3) Gatteschi, D.; Caneschi, A.; Pardi, L.; Sessoli, R. *Science* **1994**, *265*, 1054.
(4) Wang, L. S. In *Advanced Series in Physical Chemistry*; Vol. 10, Chapter XX (to be published).
(5) Fan, J.; Wang, L. S. *J. Chem. Phys.* **1995**, *102*, 8714.
(6) Wu, H.; Desai, S. R.; Wang, L. S. *J. Am. Chem. Soc.* **1996**, *118*, 5296. Table 1 corrected for entries of FeO_4 is placed in: *J. Am. Chem. Soc.* **1996**, *118*, 7434.
(7) Engelking, P. C.; Lineberger, W. C. *J. Chem. Phys.* **1977**, *66*, 5054.
(8) Andersen, T.; Lykke, K. R.; Neumark, D. M.; Lineberger, W. C. *J. Chem. Phys.* **1987**, *86*, 1858.
(9) Wang, L. S.; Wu, H.; Desai, S. R. *Phys. Rev. Lett.* **1996**, *76*, 4853.
(10) Dolg, M.; Wedig, U.; Stoll, H.; Preuss, H. *J. Chem. Phys.* **1987**, *86*, 2123.
(11) Gutsev, G. L.; Boldyrev, A. I. *Chem. Phys. Lett.* **1984**, *108*, 255.
(12) Audette, R. J.; Quail, J. W.; Black, W. H.; Roberston, B. E. *J. Solid State Chem.* **1973**, *8*, 43.
(13) Guenzburger, D.; Esquivel, D. M. S.; Danon, J. *Phys. Rev. B* **1978**, *18*, 4561.
(14) Deeth, R. J. *J. Chem. Soc., Faraday Trans.* **1993**, *89*, 3745.
(15) Deeth, R. J. *J. Chem. Soc., Faraday Trans.* **1994**, *90*, 3237.
(16) West, J. B.; Broida, H. P. *J. Chem. Phys.* **1975**, *62*, 2566.
(17) Green, D. W.; Reedy, G. T.; Kay, J. G. *J. Mol. Spectrosc.* **1979**, *78*, 257.
(18) Murad, E. *J. Chem. Phys.* **1980**, *73*, 1381.
(19) Cheung, A. S. C.; Gordon, R. M.; Merer, A. J. *J. Mol. Spectrosc.* **1981**, *87*, 289.
(20) Cheung, A. S. C.; Lee, N.; Lyyra, A. M.; Merer, A. J.; Taylor, A. W. *J. Mol. Spectrosc.* **1982**, *95*, 213.
(21) Steimle, T. C.; Nachman, D. F.; Shirley, J. E.; Merer, A. J. *J. Chem. Phys.* **1989**, *90*, 5360.
(22) Drechsler, G.; Boesl, U.; Bässmann, C.; Schlag, E. W. *J. Chem. Phys.* **1997**, *107*, 2284.
(23) Bagus, P. S.; Preston, H. J. T. *J. Chem. Phys.* **1972**, *59*, 2986.
(24) Krauss, M.; Stevens, W. J. *J. Chem. Phys.* **1985**, *82*, 5584.
(25) Bauschlicher, C. W., Jr.; Langhoff, S. R.; Komornicki, A. *Theor. Chim. Acta* **1990**, *77*, 263.
(26) Dobrodey, N. V.; Luniakov, Yu. V. *Phys. Rev. A* **1995**, *51*, 1057.
(27) Bauschlicher, C. W., Jr.; Maitre, P. *Theor. Chim. Acta* **1995**, *90*, 189.
(28) Abramowitz, S.; Acquista, N.; Levin, I. W. *Chem. Phys.* **1977**, *50*, 423.
(29) Chang, S.; Blyholder, G.; Fernandez, J. *Inorg. Chem.* **1981**, *20*, 2813.
(30) Fantarillo, M.; Cribb, H. E.; Greene, A. J.; Almond, M. J. *Inorg. Chem.* **1992**, *31*, 2962.
(31) Andrews, L.; Chertihin, G. V.; Ricca, A.; Bauschlicher, C. W., Jr. *J. Am. Chem. Soc.* **1996**, *118*, 467.
(32) Chertihin, G. V.; Saffel, W.; Yustein, J. T.; Andrews, A.; Neurock, M.; Ricca, A.; Bauschlicher, C. W., Jr. *J. Phys. Chem.* **1996**, *100*, 5261.
(33) Lyne, P. D.; Mingos, D. M. P.; Ziegler, T.; Downs, A. J. *Inorg. Chem.* **1993**, *32*, 4785.
(34) Becke, A. D. *Phys. Rev. A* **1988**, *38*, 3098.
(35) Perdew, J. P.; Wang, Y. *Phys. Rev. B* **1991**, *45*, 13244.
(36) Gutsev, G. L.; Reddy, B. V.; Khanna, S. N.; Rao, B. K.; Jena, P. *Phys. Rev. B* **1998**, *58*, 14131.
(37) Gutsev, G. L.; Rao, B. K.; Jena, P.; Wang, X. B.; Wang, L. S. Submitted for publication.
(38) Frisch, M. J.; Trucks, G. W.; Schlegel, H. B.; Gill, P. M. W.; Johnson, B. G.; Robb, M. A.; Cheeseman, J. R.; Keith, T.; Petersson, G. A.; Montgomery, J. A.; Raghavachari, K.; Al-Laham, M. A.; Zakrzewski, V. G.; Ortiz, J. V.; Foresman, J. B.; Cioslowski, J.; Stefanov, B. B.; Nanayakkara, A.; Challacombe, M.; Peng, C. Y.; Ayala, P. Y.; Chen, W.; Wong, M. W.; Andres, J. L.; Replogle, E. S.; Gomperts, R.; Martin, R. L.; Fox, D. J.; Binkley, J. S.; Defrees, D. J.; Baker, J.; Stewart, J. P.; Head-Gordon, M.; Gonzalez, C.; Pople, J. A. Gaussian 94, Revision B.1; Gaussian, Inc.: Pittsburgh, PA, 1995.
(39) Kohn, W.; Sham, L. J. *Phys. Rev.* **1965**, *140*, A1133.
(40) Gunnarsson, O.; Lundqvist, B. I. *J. Chem. Phys.* **1976**, *13*, 4274.
(41) Gross, E. K. U.; Oliveira, L. N.; Kohn, W. *Phys. Rev. A* **1988**, *37*, 2809.
(42) Löwdin, P.-O. *Phys. Rev.* **1955**, *97*, 1474.
(43) Purvis, G. D., III; Sekino, H.; Bartlett, R. J. *Col. Czech. Chem. Commun.* **1988**, *53*, 2203.
(44) Chen, W.; Schlegel, H. B. *J. Chem. Phys.* **1994**, *101*, 5957.
(45) Wang, J.; Becke, A. D.; Smith, V. H., Jr. *J. Chem. Phys.* **1985**, *102*, 3477.
(46) Cramer, C. J.; Dulles, F. J.; Giesev, D. J.; Almlöf, J. *Chem. Phys. Lett.* **1995**, *245*, 165.
(47) Görling, A.; Trickey, S. B.; Gisdakis, P.; Rösh, N. *Topics in Organometallic Chemistry*; Hoffmann, P., Brown, J. M., Eds.; Springer: Heidelberg, 1999; Vol. 4, pp 109−165.
(48) Wittbrodt, J. M.; Schlegel, H. B. *J. Chem. Phys.* **1996**, *105*, 6574.
(49) Smart, J. S. *Effective field theories of magnetism*; W. B. Saunders Co.: Philadelphia, 1966.
(50) Mulliken, R. S. *J. Chem. Phys.* **1955**, *23*, 1833.
(51) Reed, A. E.; Curtiss, L. A.; Weinhold, F. *Chem. Rev.* **1988**, *88*, 899.
(52) Zheng, H. *Phys. Rev. B* **1993**, *48*, 14868.
(53) Clementi, E.; Chakravorty, S. J. *J. Chem. Phys.* **1990**, *93*, 2591.
(54) Gill, P. M. W.; Johnson, B. G.; Pople, J. A. *Int. J. Quantum Chem. Symp.* **1992**, *26*, 319.
(55) Oliphant, N.; Bartlett, R. J. *J. Chem. Phys.* **1994**, *100*, 6550.
(56) Sekino, H.; Oliphant, N.; Bartlett, R. J. *J. Chem. Phys.* **1994**, *101*, 7788.
(57) Becke, A. D. *J. Chem. Phys.* **1993**, *98*, 5648.
(58) Stevens, P. J.; Devlin, F. J.; Chablowski, C. F.; Frisch, M. J. *J. Phys. Chem.* **1994**, *98*, 11623.
(59) Slater, J. C. *Phys. Rev.* **1951**, *81*, 385.
(60) Lee, C.; Yang, W.; Parr, R. G. *Phys. Rev. B* **1988**, *37*, 785.
(61) Vosko, S. H.; Wilk, L.; Nusair, M. *Can. J. Chem.* **1980**, *58*, 1200.
(62) Bauschlicher, C. W., Jr. *Chem. Phys. Lett.* **1995**, *246*, 40.
(63) Gutsev, G. L.; Jena, P.; Bartlett, R. J. *J. Chem. Phys.* **1999**, *110*, 403.
(64) Klobukowski, M.; Diercksen, G. H. F.; Garćia de la Vega, J. M. *Adv. Chem. Phys.* **1997**, *28*, 189.
(65) Klein, A.; McGinnis, R. P.; Leone, S. R. *Chem. Phys. Lett.* **1983**, *100*, 475.
(66) Huber, K. P.; Herzberg, G. *Constants of Diatomic Molecules*; Van Nostrand-Reinhold: New York, 1979.
(67) Schulz, G. J. *Rev. Mod. Phys.* **1973**, *45*, 423.
(68) Gutowski, M.; Simons, J. *J. Chem. Phys.* **1990**, *93*, 2546.
(69) Schröder, D.; Fiedler, A.; Schwarz, J.; Schwarz, H. *Inorg. Chem.* **1994**, *33*, 5094.
(70) Gutsev, G. L.; Rao, B. K.; Jena, P. Manuscript in preparation.
(71) Hoppe, M. L.; Schlemper, E. O.; Murmann, R. K. *Acta Crystallogr. B* **1982**, *38*, 2237.
(72) Deng, L.; Ziegler, T. *Organometallics* **1996**, *15*, 3011.
(73) Debnath, R. *Chem. Phys. Lett.* **1998**, *291*, 231.
(74) Herzberg, G. *Molecular Spectra and Molecular Structure. II. Infrared and Raman Spectra of Polyatomic Molecules*; Van Nostrand: New York, 1945; p 207.
(75) Cotton, F. A.; Wilkinson, G. *Advanced Inorganic Chemistry*; Wiley-Interscience: New York, 1988.
(76) Wang, X. B.; Ding, C. F.; Wang, L. S.; Boldyrev, A. I.; Simons, J. *J. Chem. Phys.* **1999**, *110*, 4763.
(77) Gutsev, G. L.; Boldyrev, A. I. *Adv. Chem. Phys.* **1985**, *61*, 169.
(78) Gutsev, G. L.; Bartlett, R. J.; Compton, R. N. *J. Chem. Phys.* **1998**, *108*, 6756.

(79) Gutsev, G. L.; Bartlett, R. J. *Mol. Phys.* **1998**, *94*, 121.
(80) Hotop, H.; Lineberger, W. C. *J. Phys. Chem. Ref. Data* **1985**, *14*, 731.
(81) Gelotta, R. H.; Bennet, R. A.; Hall, J. L.; Siegel, M. W.; Levine, J. *Phys. Rev. A* **1972**, *6*, 631.
(82) Simons, J.; Jordan, K. D. *Chem. Rev.* **1987**, *87*, 535.
(83) Kalcher J.; Sax, A. F. *Chem. Rev.* **1994**, *94*, 2291.
(84) Gutsev, G. L.; Boldyrev, A. I. *Chem. Phys.* **1981**, *56*, 277.
(85) Gutsev, G. L.; Khanna, S. N.; Rao, B. K.; Jena, P. To be submitted.
(86) Knight, L. B.; Babb, R.; Ray, M.; Banisauskas, T. J., III; Russon, L.; Dailey, R. S.; Davidson, E. R. *J. Chem. Phys.* **1996**, *105*, 10237.
(87) Veliah, S.; Xiang, K. H.; Pandey, R.; Recio, J. M.; Newsam, J. M. *J. Phys. Chem.* **1998**, *102*, 1126.
(88) Gutsev, G. L.; Bartlett, R. J.; Boldyrev, A. I.; Simons, J. *J. Chem. Phys.* **1997**, *108*, 3867.
(89) Gutsev, G. L.; Jena, P.; Bartlett, R. J. *Chem. Phys. Lett.* **1998**, *292*, 289.
(90) Kölmel, C.; Palm, G.; Ahlrichs, R.; Bar, M.; Boldyrev, A. I. *Chem. Phys. Lett.* **1990**, *173*, 151.
(91) Tschumper, G. S.; Fermann, J. T.; Schaefer, H. F., III *J. Chem. Phys.* **1996**, *104*, 3676.